Arthropod Structure & Development 91 (2026) 101507

Contents lists available at ScienceDirect

Arthropod Structure & Development

journal homepage: www.elsevier.com/locate/asd

The first comparison of the sperm ultrastructure of Lymexyloidea with Mordelloidea and Tenebrionoidea (Coleoptera)

Jan Batelka [a], David Mercati [b], Mariangela Gentile [b], Pietro Lupetti [b], Romano Dallai [b,*]

[a] Nad vodovodem 16, Praha, 10, Czech Republic
[b] Department of Life Sciences, University of Siena, Siena, Italy

ARTICLE INFO

Article history:
Received 5 September 2025
Received in revised form
21 November 2025
Accepted 1 January 2026
Available online 9 February 2026

Handling Editor: X Xiaoya Ma

Keywords:
Beetle sperm structure
Insect ultrastructure
Insect phylogeny

ABSTRACT

The work has considered the sperm structure of Lymexyloidea to test the relationship of this group with Tenebrionoidea and the recently proposed "Mordelloid clade", consisting of the families Mordellidae and Ripiphoridae. The sperm structure of the Hylecoetidae *Elateroides dermestoides* partially supports the above mentioned relationship as it has a short sperm provided with a peculiar acrosome characterized by an electron-dense ring at half-length and a dot at the apex. The Mordellidae species examined, *Curtimorda maculosa* and *Conalia baudii* share the unique organization of the posterior flagellar region provided with only the 9 axonemal accessory tubules. Moreover, due to the sperm length, sperm looping is evident. The Ripiphoridae *Pelecotoma fennica* exhibits notably differences from Mordellidae species lacking the unusual structure of the flagellar posterior region. The sperm looping is, however, still evident.

The large and diversified group of Cucujiformia beetles includes several superfamilies (Stork et al., 2015; Robertson et al., 2015; Bouchard et al., 2017; Goczał et al., 2024), but the relationship between them remain unresolved (McKenna et al., 2015; Zhang et al., 2018; Cai et al., 2022; Goczał et al., 2024; Li et al., 2024). The superfamily Tenebrionoidea (auct.) is one of the largest and morphological complex group of beetles with more than 30,000 species described so far within Cucujiformia (Crowson, 1966; Lawrence and Newton, 1995; Beutel and Friederich, 2005; Hunt et al., 2007). One of the phylogenetic problem in this group is the relationships of the Tenebrionoidea + Lymexyloidea as the monophyly of the latter superfamily was moderately supported according to Zhang et al. (2018), but well supported by Bocak et al. (2014) and Gunter et al. (2014). Another unresolved question involves the interrelationships between Lymexyloidea, Ripiphoridae and Tenebrionoidea. The recent phylogenomic analyses suggested Lymexyloidea as a sister group of the Tenebrionoidea (including Mordellidae and Ripiphoridae) (Zhang et al., 2018; McKenna et al., 2019; Cai et al., 2022; Li et al., 2024). As for the position of Ripiphoridae, it has traditionally been considered part of, or closely related to, Mordellidae (Lacordaire, 1859). The group was retained to have a close relationship with Meloidae on the basis of a similar wing venation and triungulin–like first instar (Forbes, 1926; Beutel and Friederich, 2005), but this hypothesis was rejected by molecular phylogenetic analyses and sperm structure (Dias et al., 2022a, 2022b). Recent morphological data and molecular phylogenetic analyses recovered the Ripiphoridae, together with Mordellidae, as a new clade defined as “Mordelloid clade” (Batelka et al., 2025) which represents the sister group to the remaining Tenebrionoidea. Here we follow conclusion of Batelka et al. (2025) and use for this lineage a traditional term Mordelloidea based on morphological, molecular and fossil evidence.

Spermatological investigations in Mordelloidea and Tenebrionoidea have revealed considerable diversity in sperm morphology across different families (Table 1). Dias et al. (2022a, b) noted that Mordellidae and Ripiphoridae exhibit sperm cysts with a low counts compared to tenebrionoid families and contain long sperm that undergo looping within germ cysts, resulting in cross-sectioning the presence of two levels of the same sperm bundles. Contrary to this arrangement, in Tenebrionoidea, which are characterized by relatively short sperm, the sperm within the germ cysts are arranged in two groups with antiparallel orientation (Dias et al., 2012, 2013a, 2013b, 2015, 2021, 2022a, 2013b, b; Folly et al., 2021, Rezende et al., 2024b).

* Corresponding author.
E-mail addresses: janbat@centrum.cz (J. Batelka), david.mercati@unisi.it (D. Mercati), mariangela.gentile@unisi.it (M. Gentile), pietro.lupetti@unisi.it (P. Lupetti), romano.dallai@unisi.it (R. Dallai).

https://doi.org/10.1016/j.asd.2026.101507

In the present work we describe, for the first time, the sperm ultrastructure of a member of Lymexyloidea (*Elateroides dermestoides*) contributing to the understanding of the group's phylogenetic affinities with Mordelloidea and Tenebrionoidea. Furthermore, we expand the observation to other members of Ripiphoridae and Mordellidae, aiming to validate previous ultrastructural findings, supporting the sister relationship of the Mordelloidea and Tenebrionoidea.

1. Material and methods

The following species (Fig. 1) were studied for the present work:

- Lymexyloidea: Hylecoetidae: *E. dermestoides* (Linnaeus, 1761); Czech Republic, 30 km E of Praha, Jevany env., April 2024, 2025.
- Mordelloidea: Mordellidae: *Curtimorda maculosa* (Neazen, 1794); Czech Republic, 25 km E of Praha, Vyžlovka env., June 2025, ex. larva from fruit bodies of polyporous fungus *Gloeophyllum* sp.
- Mordelloidea: Mordellidae: *Conalia baudii* Mulsant and Rey, 1858; Czech Republic, Praha – Dubeč, July 2025.
- Mordelloidea: Ripiphoridae: *Pelecotoma fennica* (Paykull, 1799); Czech Republic, Praha – Lipence, July 2025.

All specimens collected by Jan Batelka.

1.1. Fluorescence microscopy

Sperm (spermatozeugmata) of *E. dermestoides* were taken from the last part of deferent ducts of adult males. The material was placed over a glass in a small drop of 0.1 M phosphate buffer (pH 7.2) to which 3 % of sucrose was previously added (PB). The sperm bundles were squashed with a coverslip and observed and photographed using interference contrast and epifluorescent microscopy with a Leica DMRB microscope equipped with AxioCam HR camera (Carl Zeiss). DNA was stained for fluorescence observations by incubating the sperm bundles for 3–4 min in Hoechst 33258 1 μg/ml (Sigma). The material was then mounted in a drop of 90 % glycerol.

1.2. Transmission electron microscopy

Males were dissected in 0.1 M phosphate buffer (PB), pH 7.2, with 3 % of sucrose. After dissection, the whole reproductive system was removed and the testes, deferent ducts and seminal vesicles were isolated. The material was fixed overnight in 2.5 % glutaraldehyde in PB at 4 °C. After rinsing in PB, the material was post-fixed for 2 h in 1 % of osmium tetroxide in PB at 4 °C. After rinsing in PB, the material was dehydrated in an ascending alcohol series, then transferred into propylene oxide and finally embedded in Epon-Araldite resin mixture. Ultrathin sections (50–60 nm), obtained with a Reichert Ultracut ultramicrotome equipped with a diamond knife, were mounted upon copper grids, stained routinely with uranyl acetate and lead citrate, and then observed

Table 1
Spermatological studies of Lymexyloidea, Mordelloidea and Tenebrionoidea.

Lineage	Taxon	Origin	Source
Lymexyloidea			
Hylecoetidae	*Elateroides dermestoides*	Czech Republic	this study
Mordelloidea			
Mordellidae	*Conalia baudii*	Czech Republic	this study
Mordellidae	*Curtimorda maculosa*	Czech Republic	this study
Mordellidae	*Hoshihananomia* sp.	Brazil	Dias et al. (2022b)
Mordellidae	*Mordellistena* sp.	Italy	Dias et al. (2022a)
Mordellidae	*Mordellistena brevicauda*	Italy	Dias et al. (2022b), Dallai et al. (2024)
Ripiphoridae	*Macrosiagon tricuspidata*	Spain	Nardi et al. (2013)
Ripiphoridae	*Pelecotoma fennica*	Czech Republic	Kathirithamby et al. (1993), this study
Ripiphoridae	*Ptilophorus dufourii*	Italy	Dallai (2014), Dias et al. (2022a)
Tenebrionoidea			
Ciidae	*Ceracis cornifer*	Brazil	Folly et al. (2021)
Meloidae	*Berberomeloe* sp.	Spain	Afzelius and Dallai (1994)
Meloidae	*Berberomeloe majalis*	Italy	Dias et al. (2022a)
Meloidae	*Hycleus scutellatus*	Spain	Nardi et al. (2013)
Meloidae	*Lytta vesicatoria*	Italy	Afzelius and Dallai (1994), Dias et al. (2022a)
Meloidae	*Mylabris variabilis*	Spain	Nardi et al. (2013)
Meloidae	*Mylabris variabilis*	Italy	Dias et al. (2022a)
Meloidae	*Mylabris hieracii*	Italy	Dias et al. (2022a)
Meloidae	*Zonitis flava*	Spain	Nardi et al. (2013)
Oedemeridae	*Oedemera nobilis*	Italy	Dias et al. (2022b)
Pythidae	*Pytho depressus*	Italy	Dias et al. (2021)
Scraptiidae	*Anaspis lurida*	unknown	Rezende et al. (2024a)
Scraptiidae	*Anaspis pulicaria*	unknown	Rezende et al. (2024a)
Tenebrionidae	*Accanthopus velikensis*	Italy	Dias et al. (2022b)
Tenebrionidae	*Blaps polycresta*	Egypt	Shonouda and Osman (2018)
Tenebrionidae	*Blaps sulcata*	Egypt	Kheirallah et al. (2017)
Tenebrionidae	*Lagria villosa*	Brazil	Dias et al. (2013a, b)
Tenebrionidae	*Palembus dermestoides*	unknown	Dias et al. (2012)
Tenebrionidae	*Palembus dermestoides*	Brazil	Almeida and Cruz-Landim, 2000
Tenebrionidae	*Phaleria testacea*	Brazil	Rezende et al. (2024b)
Tenebrionidae	*Tachyderma hispida*	Egypt	Kheirallah et al. (2016)
Tenebrionidae	*Tenebrio molitor*	Italy	Afzelius and Dallai (1994)
Tenebrionidae	*Tenebrio molitor*	unknown	Dias et al. (2012)
Tenebrionidae	*Tribolium castaneum*	unknown	Dias et al. (2012, 2015)
Tenebrionidae	*Zophobas confusa*	unknown	Dias et al. (2012)

Fig. 1. Representatives of the investigated lineages and their natural habitats. **A)** Fallen *Fagus sylvatica* infested by lymexyloid *Elateroides dermestoides,* **B)** male, **C)** female. **D–G)** Habitat of mordellid *Conalia baudii* (in the circle) in house gardens. **D)** Parts of dried-up log of *Pseudotsuga menziesii* devoid of bark. **E)** Ibidem, crevice with running *Conalia baudii*. **F)** Rotten log of *Picea abies* inhabited by mordellids *Conalia baudii* and *Curtimorda maculosa.* **G)** Ibidem, ventral view on fruit bodies of polyporous fungus *Gloeophyllum* sp. **H)** Partially dead tree *Populus nigra* inhabited by the wood–boring beetle *Ptilinus fuscus* and its ripiphorid parasite *Pelecotoma fennica* (male in the circle). Photographs were taken in Czech Republic, central Bohemia, 2025 by J. Batelka.

with a Philips CM10 transmission electron microscope operating at an accelerating voltage of 80 kV.

2. Results

2.1. Lymexyloidea - Hylecoetidae

2.1.1. E. dermestoides

The sperm of this species is relatively short, measuring approximately 76–80 μm in length (Fig. 2A and B). The apical acrosome is flattened and measures 1.25–1.33 μm in length (Fig. 2F). In longitudinal section, the acrosome, has a conical shape and shows an axial perforatorium that does not reach the tip (Fig. 2C–E). Its large basal region is housed in a cavity of the nuclear anterior region (Fig. 2E). Notably, at about half acrosome length, an unexpected thin electron-dense ring (65 nm wide on a side and only 16 nm on the opposite side) is present beneath the plasma membrane (Fig. 2C–E). A cross section of the acrosome at this level

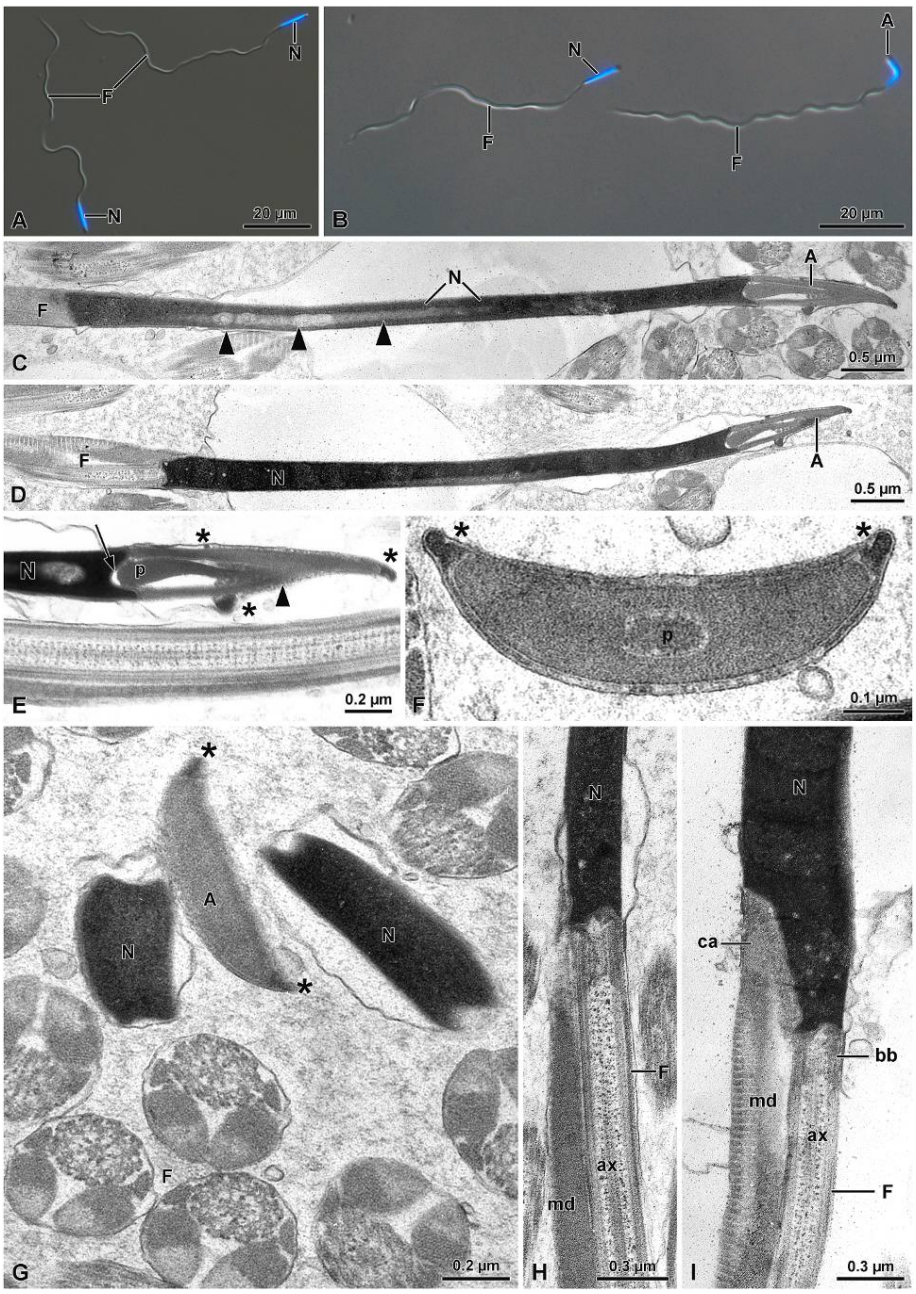

Fig. 2. *Elateroides dermestoides*. **A-B)** Sperm after fluorescent Hoechst staining. Note the apical acrosome (A), the fluorescent nucleus (N) and the flagellum (F). **C)** Longitudinal section of the sperm head with the conical acrosome (A) and the apparently cylindrical nucleus (N). Note the nuclear inner cavity (arrowheads) F, flagellum. **D**) Longitudinal section of a long sperm head. Note the identical structure of the acrosome (A). N, nucleus; F, flagellum. **E)** Detail of the acrosome (A) with the thick perforatorium (p) that apically ends before acrosomal apex (arrowhead). Basally it is adapted in a nuclear (N) small cavity (arrow). Note the ring of electron-dense material at half acrosome length and at the acrosome tip (asterisks). **F)** Cross section through the acrosome (A) at the level of the electron-dense ring (arrowheads). p, perforatorium. **G)** Cross section of the rectangular nuclear (N), the acrosome (A) at the level of the electron-dense ring (asterisks) and some sperm flagella (F). **H-I)** Longitudinal sections through the transition region between nucleus (N) and flagella (F). ax, axoneme; bb, basal body; ca, centriole adjunct material; md, mitochondrial derivatives.

(0.75 µm in diameter) clearly shows the position of this electron-dense material (Fig. 2F). At the acrosomal tip a further small electron-dense dot (75 nm long) is also present (Fig. 2C–E). The nucleus can vary in length (Fig. 2C and D), ranging from about 5.5 to 6.3 µm long; it has an unusual rectangular outline in cross section (0.66 µm × 0.25 µm) (Fig. 2G and 3A). Longitudinal sections often reveal chromatin-free zones (Fig. 2C). Posteriorly, the nucleus narrows, maintaining, however, a rectangular profile (0.3 µm wide) (Fig. 2G). The posterior nuclear region has a flute beak shape; on a side of the region, the two mitochondrial derivative begin to appear, while, on the opposite side, the basal body and the flagellar axoneme are visible (Fig. 2H and I; 3A). The axoneme consists of the common 9 + 9+2 microtubular pattern, accompanied by two equal elliptical mitochondrial derivatives, with their region facing the axoneme denser and crystallized (Fig. 3B). Two elongated elliptical accessory bodies flank the axoneme (Fig. 3B). Cross sections frequently show grouped flagella with either clockwise or counterclockwise axoneme orientations (Fig. 3C and D). Posteriorly, both mitochondrial derivatives and accessory bodies reduce in diameter and then disappear; the axoneme ends

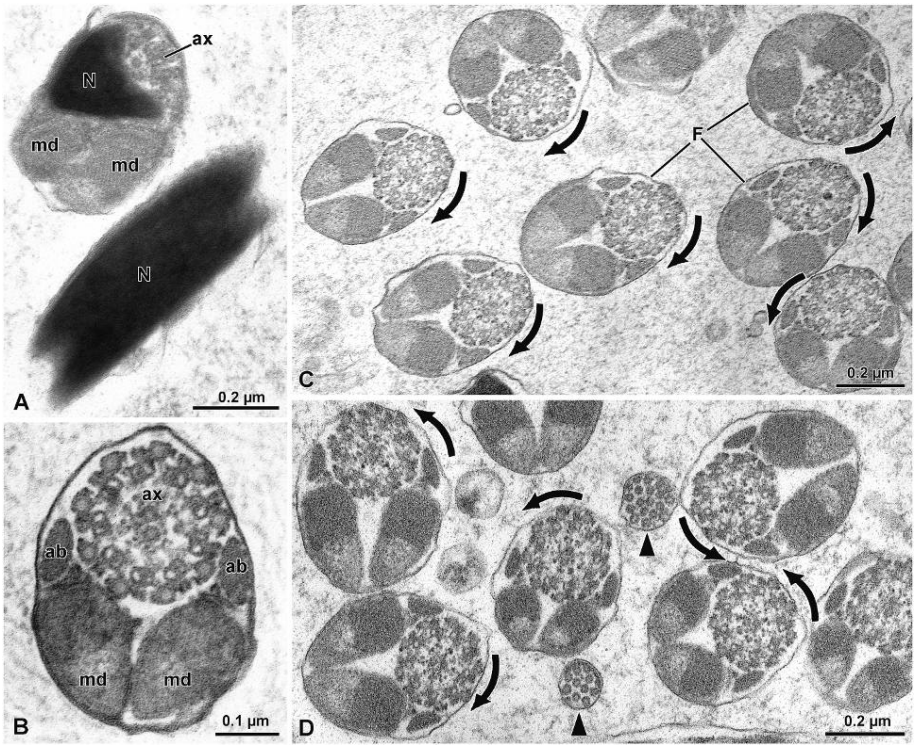

Fig. 3. *Elateroides dermestoides*. **A)** Cross section of the transition region nucleus (N) - flagellum. Note the two mitochondrial derivatives (md) and the beginning of the axoneme (ax). A rectangular nucleus (N) is also visible. **B)** Detail of the flagellar axoneme (ax) with the 9 + 9+2, the two elliptical accessory bodies (ab) and the two equal mitochondrial derivatives (md). **C-D)** Cross sections through the sperm flagella (F) showing axonemes with opposite orientation (see arrows). Note the flagellar tail end with only singlet microtubules (arrowheads).

is a small circular structure with only a few singlet microtubules (Fig. 3D).

2.2. *Mordelloidea (= Mordelloid clade of Tenebrionoidea)*

2.2.1. *Mordellidae*

2.2.1.1. Curtimorda maculosa. This species exhibits relatively long sperm, about 1100 μm in length. As typical for insects, sperm develop within testicular germ cysts, each containing about 64 units (equivalent to 2^6 cell divisions) (Fig. 4A and B). Cross sections of the cysts frequently reveal sperm bundles appearing at two different levels: one section at the anterior flagellar region and the other at a posterior level, resulting from looping of the long flagella (Fig. 4A). When the cross-section interests the anterior sperm region, acrosome, nucleus and the beginning of flagellum of the sperm bundle are visible (Fig. 4D). The sperm has an apical conical bilayered acrosome with an axial perforatorium (Fig. 4D). The cylindrical nucleus has a diameter of 0.67 μm and, before reaching the complete maturation, contains a fine granular material. A crown of cytoplasmic microtubules surrounds the nucleus (Fig. 4C). At full maturation the nucleus becomes electron-dense, measuring 0.31 μm in diameter (Fig. 4D). The posterior nuclear region has a semilunar cross section and houses on a side the basal body and, on the opposite side, the two mitochondrial derivatives, intermingled with the electron-dense material of the centriole adjunct (Fig. 4D inset). Further posteriorly, the nucleus terminates and the two mitochondrial derivatives enlarge. On the opposite side, the flagellar axoneme appears with all its microtubular components and the two elongated elliptical and curved accessory bodies embracing the axoneme (Fig. 4E). A cross section through this level shows the sperm bundle with 64 units in orderly assemblage (Fig. 4B). The sperm bundle has an hexagonal configuration 5.7 μm wide. Each sperm at this level shows, in a cross section, a 9 + 9+2 axonemal pattern, flanked by the accessory bodies and beneath by the two globular mitochondrial derivatives of unequal diameter, that on the left side larger (0.40 μm wide) than the opposite one (0.15 μm wide) (Fig. 4E). The central region of the mitochondrial derivatives display a denser matrix compared to the periphery. The posterior flagellar region has a quite uncommon appearance compared to the anterior region. The sperm cross section of the flagellum, 0.47 μm in diameter, contains the large mitochondrial derivative and, on the opposite side, the remnant of the disorganized flagellar axoneme consisting of some microtubules (Fig. 4F). Further posteriorly, in cross section (0.40 μm wide), nine accessory tubules are arranged peripherally and embedded in an electron-dense material are recognizable (Fig. 4G and H). The flagellar end, 0.31 μm–0.21 μm wide, still shows 9 accessory tubules, some randomly distributed or in orderly axial position, always embedded in the electron-dense material (Fig. 4H). This material must be produced at sperm maturity, as it is absent in the spermatid stage (Fig. 4G).

2.2.1.2. Conalia baudii. The species, similar to other members of the family, has sperm quite long, about 1170 μm. In the testes sperm are arranged within germ cysts in a compact group showing an almost irregular hexagonal shape in a cross section (Figs. 5 and 6A-C). Each group counts about 45–50 sperm units, rather than 64, as it was expected according to the number of cell divisions within the germ cyst. This result is possibly due to the degeneration of some spermatids during spermiogenesis (Fig. 5). A cross section through a cyst often interests two levels of the same sperm group; when this occurs, if the two cross sections are through the flagellar axonemes, they show an opposite orientation; alternatively, one section of the sperm group is through the nuclear region and the

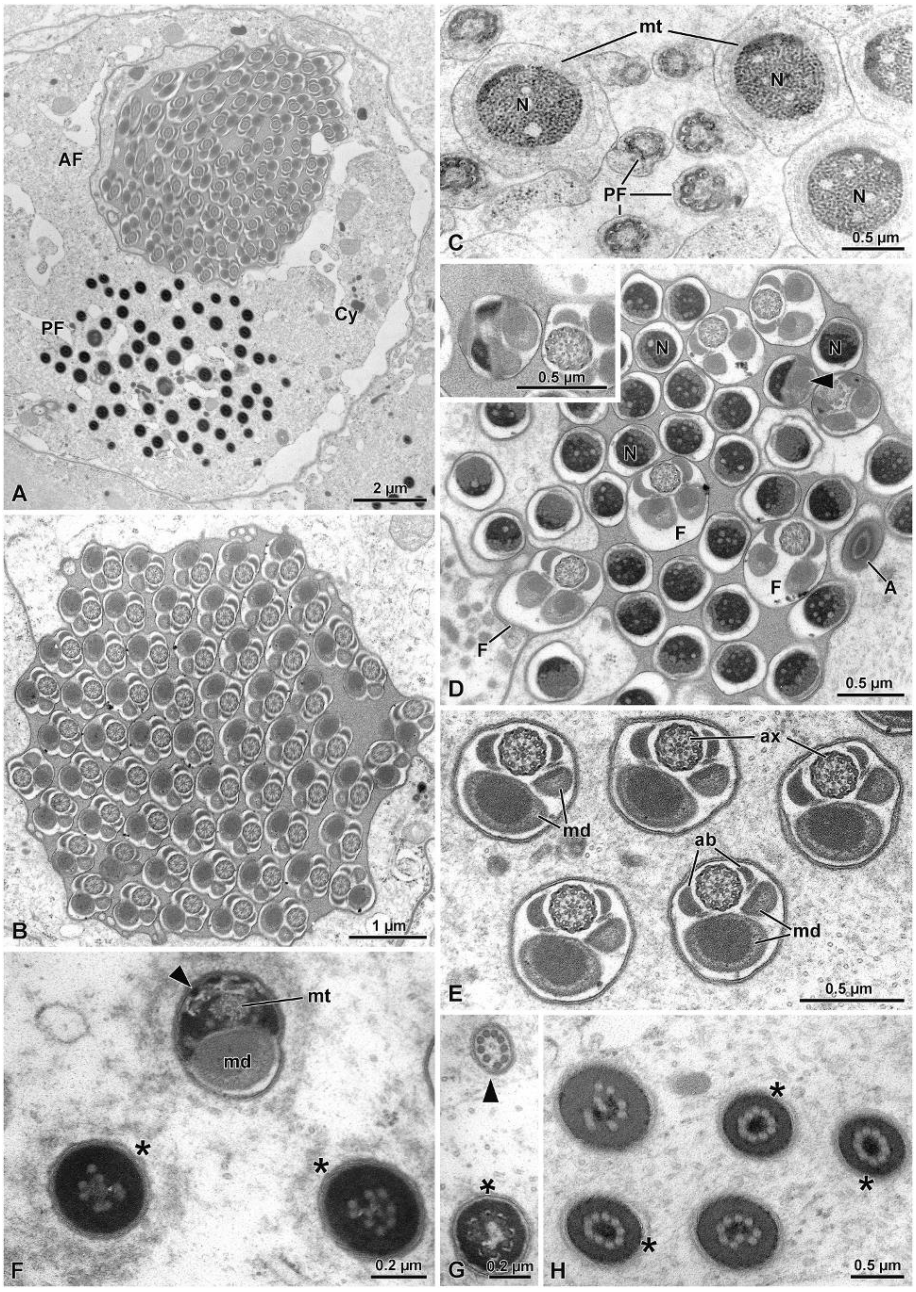

Fig. 4. *Curtimorda maculosa*. **A)** Cross section through a sperm cyst showing two levels of the same sperm bundle. The long sperm are involved in sperm looping to be contained in the reduced cyst size. Note the cross sectioned anterior flagellar region (AF) with the complete flagellar components and the posterior region (PF) provided with only accessory tubules embedded in an electron-dense material. Cy, cyst cytoplasm. **B)** Cross section of a sperm bundle with about 64 sperm flagella. Note the hexagonal shape of the sperm complex. **C)** Cross section of an immature cyst showing the nuclei (N) with fine granular material surrounded by microtubules (mt). Note the flagellar posterior region (PF) with only accessory tubules surrounded by a reduced electron-dense material. **D)** Cross section through the most anterior region of the sperm bundle. Cylindrical nuclei (N), the transition region to the flagellum (arrowhead), the acrosome (A) and some flagellar section (F) are visible. In the inset detail of the transition region between nucleus and flagellum. **E)** Cross section of the flagellar anterior region with the 9 + 9+2 axoneme (ax), the two elliptic accessory bodies (ab) embracing the axoneme and the two asymmetric mitochondrial derivatives (md). The wider mitochondrial derivative is on the left side. **F)** Cross section of the transition region between the anterior and the posterior flagellum. Note the large mitochondria derivative (md) and, on opposite side, the disorganized axoneme with the accessory tubules (arrowhead) embedded in an electron-dense material. In the axial region, remnants of microtubules are evident (mt). On the downside two sections of the posterior flagella are evident (asterisks). **G)** Further posterior cross section of the flagella after the disappearance of the mitochondrial derivative, showing 9 peripheral accessory tubules embedded in an electron-dense material (asterisk). Note on the upper side a tail tip with only 9 accessory tubules (arrowhead). This cross section is of a flagellar spermatid devoid of the electron-dense material. **H)** Detail of a cross section through the tail tip with the circle of 9 accessory tubules embedded in an electron-dense material (asterisks).

other through the flagellar posterior region, which is characterized by a peculiar flagellar structure (Fig. 6A–B). These results are the consequence of the long sperm and the occurrence of a sperm looping.

Anteriorly the sperm have a conical acrosome. In older spermatids the acrosome is 0.53 µm long and 0.37 µm wide and the perforatorium is absent (Fig. 6D). At sperm maturity the acrosome has a diameter of 0.31 µm at the basal region and only 0.21 µm at the apex, and it is filled with electron-dense material (Fig. 6E). A thin space, filled with fine granular material, is present between the sperm outer plasma membrane and the acrosomal membrane (Fig. 6E). According to this configuration, the acrosome can be

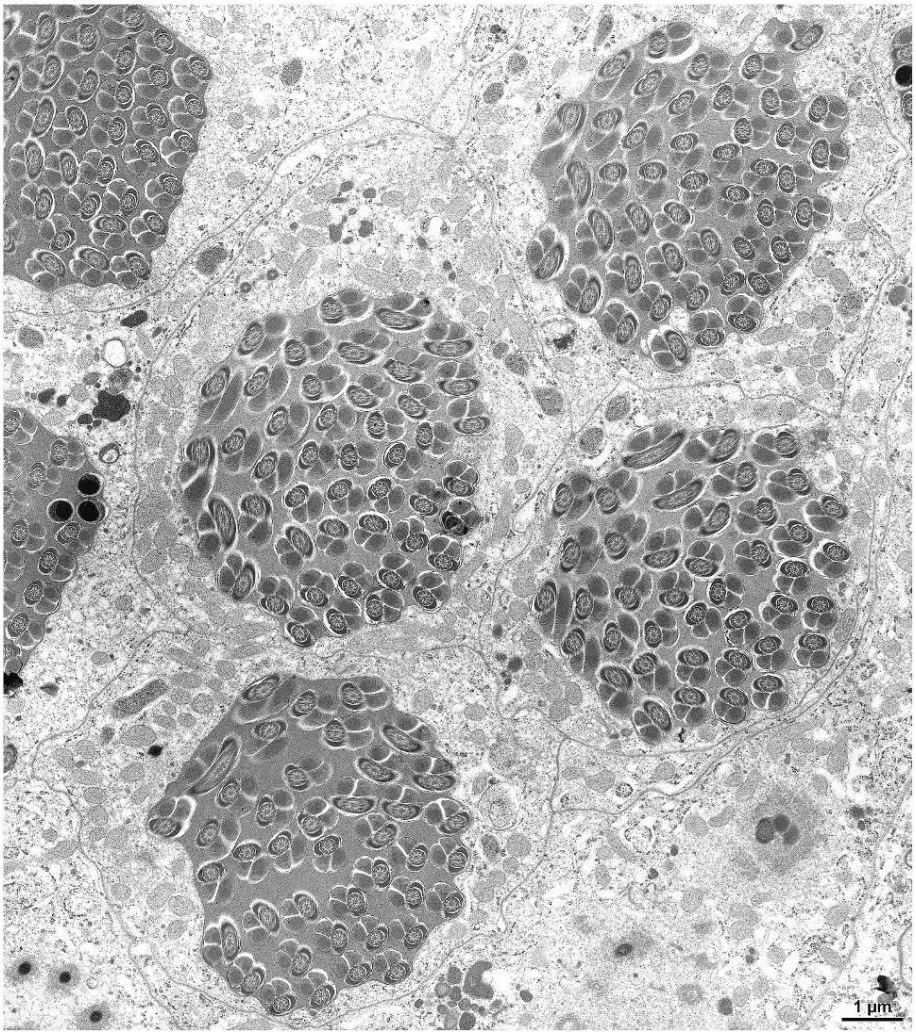

Fig. 5. *Conalia baudii*. Cross section through several sperm cysts showing flagellar regions with a number of units lower than that expected. Possibly this is due to the spermatid degeneration during spermiogenesis.

defined as provided with a three-layered structure. The cylindrical nucleus has a diameter of 0.31 µm and it is filled with electron-dense chromatin, but it also shows a peripheral region with a granular texture (Fig. 6A–C). The posterior nuclear region, in cross section, has a triangular structure well adapted between two small mitochondrial derivatives (Fig. 6F). When the nucleus ends, the basal body takes its place (Fig. 6G). Two accessory bodies are lateral to the structure, while on the opposite side, the two small mitochondrial derivatives are visible (Fig. 6G). Further posteriorly, the flagellar axoneme takes the expected 9 + 9+2 microtubular pattern with the two elongated accessory bodies embracing the structure (Fig. 7A). In a position opposite to the axoneme, two asymmetric mitochondrial derivatives are present, with that on the left side a little larger than the opposite one (Fig. 7A).

Towards the posterior sperm region, the flagellar structure undergoes dramatic changes. The axoneme degenerates, and an electron-dense material expands in its place. In a cross section, only the 9 outer accessory tubules are recognizable, with a single mitochondrial derivative present on the opposite side (Fig. 7B–C). Further, also this mitochondrion disappears, and the flagellum reduces its diameter to 0.51 µm and further to only 0.21 µm (Fig. 7D–E). The electron-dense material embedding the accessory tubules is produced during the final steps of spermiogenesis, when the accessory tubules are still visible (Fig. 7B).

2.3. Ripiphoridae

2.3.1. Pelecotoma fennica

Testes of *P. fennica* contain numerous sperm cysts, each with approximately 110–120 sperm (presumably resulting from 2^7 cell divisions) (Fig. 8A). In several sections nearby sperm bundles are fuse, forming large cluster with over 200 sperm units (Fig. 8B). As in Mordellidae, cross-sections of the same sperm cyst, often show two distinct levels of the same sperm bundle due to the sperm looping of the long sperm (Fig. 8C–D). As consequence, the two sperm axonemes in the two groups have an opposite orientation (Fig. 8D). Sperm are about 1200 µm long. The apical sperm region contains a conical acrosome, 1.10 µm long and 0.3 µm wide, showing an axial perforatorium (Fig. 9B). Towards the apex, the acrosome becomes flat, 0.40 µm wide and only 90 nm thick and contains a fine granular material (Fig. 9B–C), giving it a three-layered appearance. The perforatorium base is hosted in a small nuclear cavity (Fig. 9C). The cylindrical nucleus, 0.3 µm in diameter, is electron-dense (Fig. 9A–C) and its posterior end expands into a flute beak shape (Fig. 9A). On a side, some microtubules of the beginning flagellum are recognizable while on the opposite side, the two initial mitochondrial derivatives are emerging (Fig. 9A, inset). Further posteriorly, the complete flagellar axoneme is visible with the classic 9 + 9+2, accompanied by two small

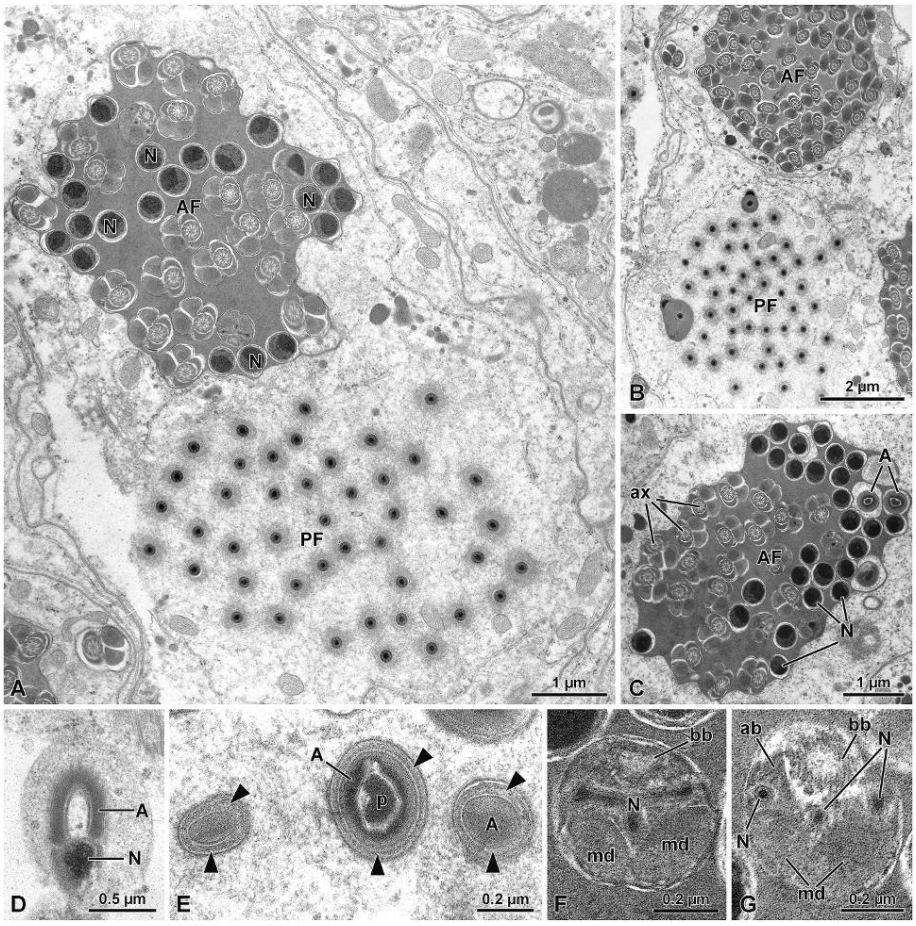

Fig. 6. *Conalia baudii.* **A)** Cross section of two levels of the same sperm complex after sperm looping. Note that in the upper region the anterior flagellar region (AF) some nuclear sections (N) are visible, while in the bottom the peculiar posterior flagellar region (PF) is present. **B)** Cross section through two levels of the sperm bundle in two different cysts. In the upper section (AF) the anterior complex of sperm flagella, embedded in an electron-dense material, is visible, while at the bottom the peculiar flagellar ends (PF) with only the accessory tubules are present. **C)** Cross section through the anterior flagellar region (AF) with axoneme (ax) and nuclei (N) embedded in an electron-dense material. **D)** Cross section of a spermatid acrosome (A). Note that the inner perforatorium is not yet visible. N, nucleus. **E)** Cross section of the acrosome at two different levels. Note that the acrosome in mature sperm has a three layered appearance, with a thin layer between the plasma membrane (arrowheads) and the acrosome (A), filled with granular material. The two small structures lateral to the acrosome are of its apex. **F)** Cross section of the transition region between nucleus (N) and flagellum. Note the two mitochondrial derivatives (md) and the basal body (bb). ab, accessory body. **G**) Cross section a little behind the previous section. Note the residues of nucleus (N), the mitochondrial derivatives (md) and the basal body (bb).

ovoidal accessory bodies, and two equal elliptical mitochondrial derivatives (0.21 μm long and 0.12 μm wide) (Fig. 9D); their region facing the axoneme has an electron-denser matrix. Posteriorly, the accessory bodies and mitochondrial derivatives taper and then disappear (Fig. 9E). The tail end has only the flagellar axoneme which progressively becomes disorganized up to exhibit only 9 accessory tubules in a narrowed triangular flagellar extremity (Fig. 9F–G).

3. Discussion

The species studied in the present work belong to the family Hylecoetidae of the superfamily Lymexyloidea and to the families Mordellidae and Ripiphoridae of the recently proposed "Mordelloid clade" of Tenebrionoidea, hereinafter referred to as Mordelloidea in accordance with Batelka et al. (2025).

The phylogenetic placement of Lymexyloidea, long debated (Hunt et al., 2007; Bocak et al., 2014; Gunter et al., 2014; Robertson et al., 2015; Timmermans et al., 2016; Liu et al., 2020; Cai et al., 2022; Li et al., 2024; McKenna et al., 2019; Zhang et al., 2018) is now accepted as a sister group to the clade Tenebrionoidea + Mordelloidea, from which it differs mainly in larval development and morphology, and 5-5-5 tarsal formula in adults (Batelka et al., 2025).

The sperm structure of the *E. dermestoides* (Hylecoetidae) here examined, partially supports this relationship. The flagellum exhibits structural features common to Mordelloidea and Tenebrionoidea including the two mitochondrial derivatives and the well-formed accessory bodies. However, a distinguishing trait is the unique organization of the flat acrosome, which includes an unusual electron-dense ring at mid-length and at the apex. Moreover, *E. dermestoides* has short sperm, like some Tenebrionoidea while on the contrary, in Mordelloidea the sperm generally is extremely long with the exception of *Mordellistena brevicauda* (Dias et al., 2022b), where sperm are of intermediate length. The short sperm likely preclude looping during sperm developing, a feature consistently observed in Mordellidae and Ripiphoridae (Dias et al., 2022a, 2022b). The short sperm length of *E. dermestoides* does not exclude, however, the possibility that the species can have sperm within the cysts arranged with an opposite orientation as it occurs in Tenebrionoidea (Dias et al., 2012, 2022a, 2022b). This arrangement was also captured in several cross

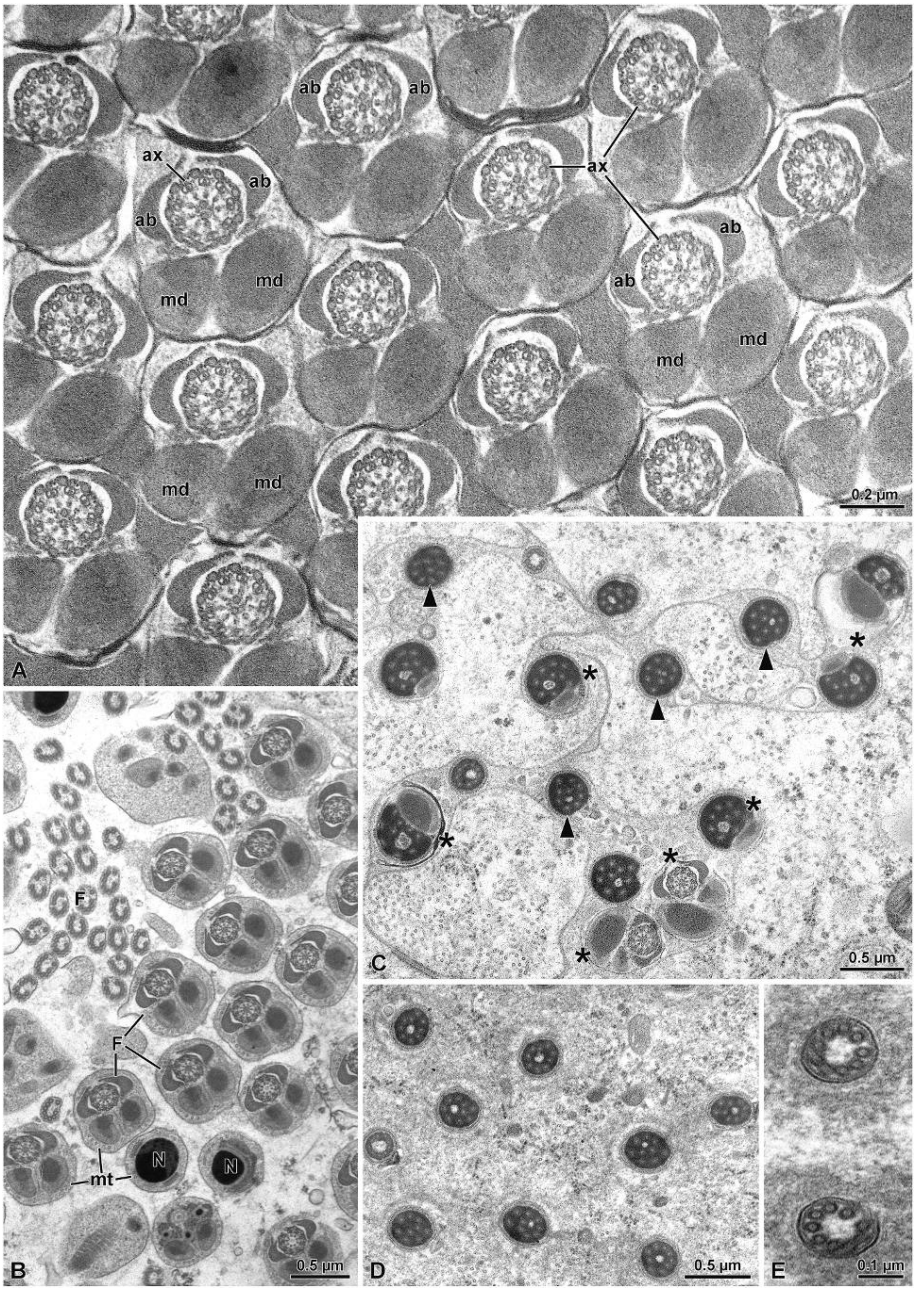

Fig. 7. *Conalia baudii*. **A)** Cross section through the sperm flagella at higher magnification. Note the 9 + 9+2 flagellar axoneme (ax), the two elongated accessory bodies (ab) embracing the axoneme and the two unequal mitochondrial derivatives (md) with that on the left side a little larger than the opposite one. **B)** Cross section of aged spermatids with sperm flagella (F), nuclei (N), both surrounded by microtubules (mt). In the upper region several sections of the flagellar end (F) are visible, each one with only accessory tubules of the axoneme, still devoid of the embedding electron-dense material. **C)** Cross section of the transition region between the conventional flagellar axoneme (asterisk) and the flagellar end with only accessory tubules (arrowheads). **D-E)** Detail of the tail tip with the 9 accessory tubules of the axoneme embedded in the electron-dense material.

sections during our study. The absence of sperm cysts in our preparations may reflect the onset of complete spermatogenesis during the pupal stage, consistent with the short lifespan of males in this species. The hypothesis of a close relationship between Lymexyloidea and Ripiphoridae + Mordellidae (Crowson, 1955; Lawrence and Newton, 1995; Bouchard et al., 2017; Cai et al., 2022) currently receives only moderate support from sperm ultrastructure. Plausible explanation could be that according to the fossil record, contrary to molecular studies, these lineages are not directly related because of stem group of Mordelloidea preceding both crown lineages of Mordelloidea (Batelka et al., 2025).

Regarding the Mordelloidea, current molecular phylogeny places it as sister to Tenebrionoidea (all remaining tenebrionoid lineages excluding Mordellidae and Ripiphoridae) (Batelka et al., 2025). Our findings reinforce this sister-group relationship based on sperm characteristics, while adding new ultrastructural details absent from earlier, partial descriptions by different authors (Kathirithamby et al., 1993; Nardi et al., 2013).

In case of Mordellidae, *C. maculosa* and *Conalia baudii* have almost the same general characteristics of the few species previously studied such as *Mordellistena* sp., *M. brevicauda* and *Hoshihananomia* sp. (Dias et al., 2022a, 2022b). The most important ultrastructural features shared by all these species with *C. maculosa* and *Co. baudii* are:

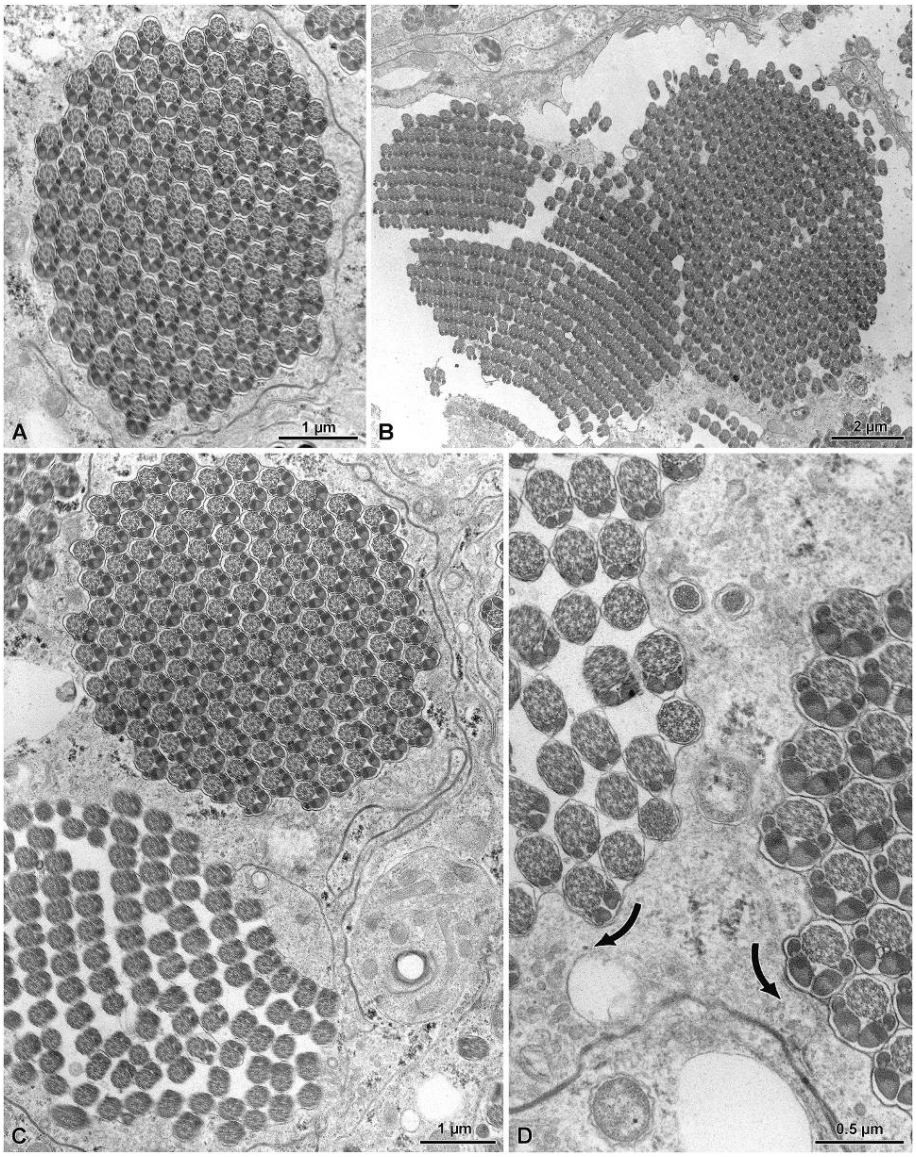

Fig. 8. *Pelecotoma fennica*. **A)** Cross section through a sperm cyst showing about 120 sperm in a compact array. The section is at the anterior flagellar region. **B)** Cross section of sperm cysts fusion giving rise to a larger complex. **C)** Cross section of a sperm cyst showing two levels of the same sperm bundle due to the its bending due to the sperm length. The upper section is through the anterior flagellar region, while the down section is instead at the posterior flagellar region with small mitochondrial derivatives. **D)** Cross section through two levels of the same sperm bundle. On the right the axoneme is sectioned at the anterior region, with flagella provided with large mitochondrial derivatives. On the left the section is through the distal flagella with axoneme showing small mitochondrial derivatives. The flagellar axonemes, in the two sections, have an opposite orientation (arrows) due to the sperm looping.

1) the unique organization of the long posterior region up to the tail end of the sperm flagella, which retains only a crown of 9 accessory tubules embedded in an electron-dense material, unlike the typical progressive reduction of the sperm components up to the complete disorganization of the axoneme at the tail end (Dallai, 2014).
2) the sperm looping within the germ cysts, a consequence of the long sperm relative to the reduction to cyst volume. Cross sections of cyst reveal two levels of the same sperm bundle, with reverse axoneme orientation (Dias et al., 2012, 2022a, 2022b).

Moreover, all the species of Mordellidae studied so far, including *C. maculosa* and *Co. baudii* produce cysts with 64 sperm cells, a trait considered ancestral compared with the higher sperm counts seen in some families of Tenebrionoidea (Dias et al., 2022a). In *Co. baudii* the sperm cysts have a more variable number of units possibly due to the degeneration of several spermatids during spermiogenesis. This challenges earlier conclusions by Virkki (1973), retaining specialized insects to have less sperm per cyst than those more primitive.

The sperm model of *Curtimorda* and *Conalia* here examined can be summarized as follows: bi-layered acrosome, cylindrical nucleus and a 9 + 9+2 flagellar axoneme in the anterior region, with two well evident triangular accessory bodies embracing the axoneme and two asymmetric roundish mitochondrial derivatives. The presence of asymmetric mitochondrial derivatives is similar to what was described for *Hoshihananomia* sp. from Brazil, while both species of Mordellistenini share symmetric mitochondrial derivatives (Dias et al., 2022b). The flagellar posterior region of *Curtimorda* and *Conalia* is provided with an uncommon structure with only 9 accessory tubules embedded in an electron-dense

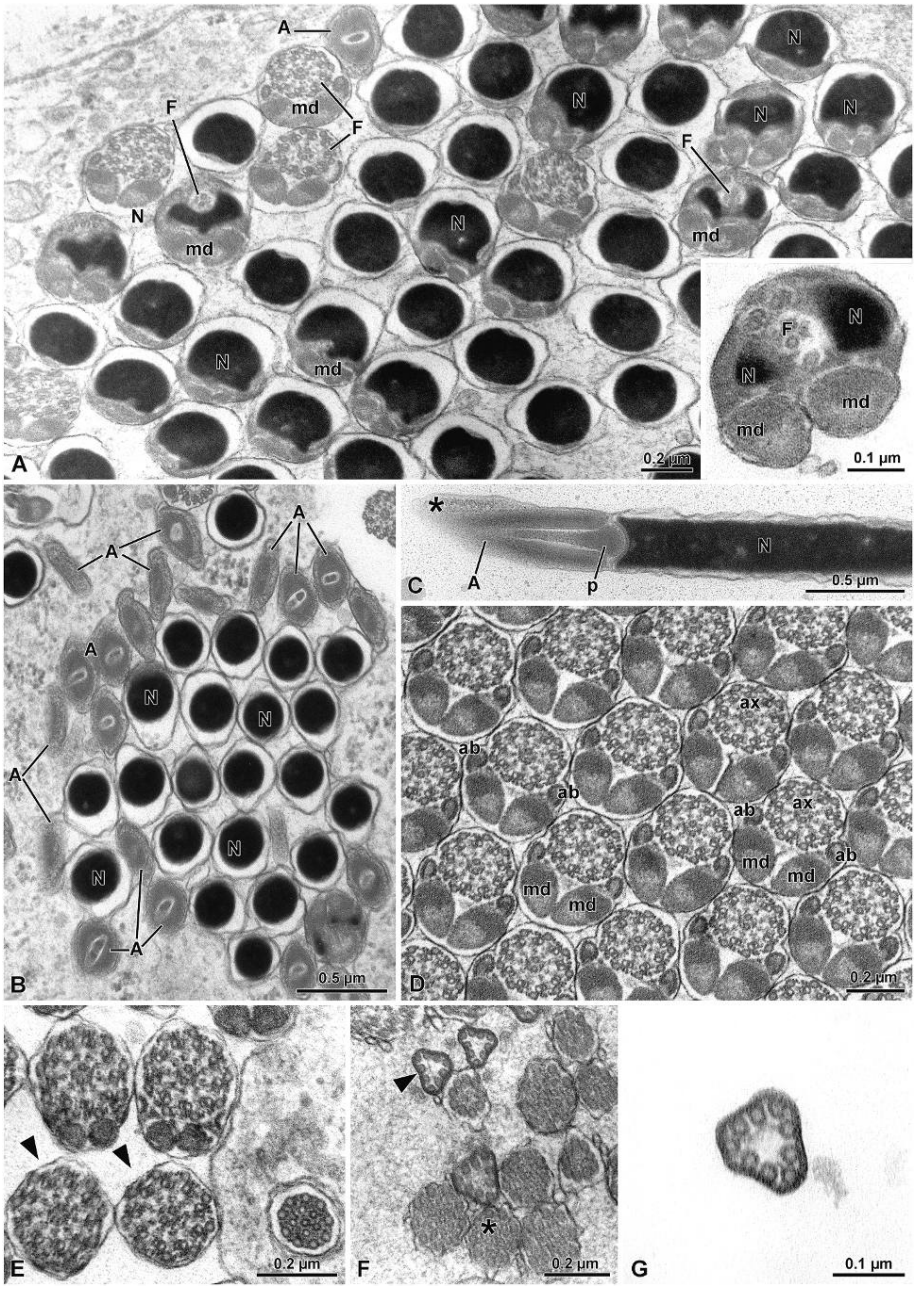

Fig. 9. *Pelecotoma fennica*. **A)** Cross section through a sperm cyst at the transition region between the nucleus and the flagellum. The posterior region of the nucleus (N) has a reduced section to host the two mitochondrial derivatives (md) on a side and the beginning of the flagella (F) on the opposite side. Sections of nucleus (N), acrosome (A) and flagella (F) are also visible. In the inset, detail of the transition region. F, flagellum; N, nucleus; md, mitochondrial derivatives. **B)** Cross section through the anterior region of a sperm cyst. Note the apical flat acrosome (A) and the cylindrical nucleus (N). **C)** Longitudinal section of the flat acrosome (A) with the inner perforatorium (p), and the apex with granular material (asterisk). N, nucleus. **D)** Cross section through the sperm flagella. Note the equal elliptical mitochondrial derivatives (md), the axoneme (ax) and the two small accessory bodies (ab). **E)** Cross section through the flagellar end without mitochondrial derivatives (arrowheads). **F)** Cross sections towards the flagellar end with disorganized axonemes (asterisk) and the flagellar tip with only accessory tubules (arrowhead). **G)** Detail of the triangular flagellar tip with only the 9 accessory tubules.

material, a pattern never found in families of Mordelloidea and Tenebrionoidea studied so far.

The ripiphorid species *P. fennica* exhibits some notably differences from Mordellidae species. It lacks the unusual posterior flagellar structure and has a higher sperm count per cyst, consistent with findings for *Macrosiagon tricuspidata* by Nardi et al. (2013). Additional, in *P. fennica*, the sperm cysts tend to fuse together to give origin to large sperm assemblage. Nonetheless, the important feature of sperm looping is still evident also in this ripiphorid species. This arrangement was also described in *Ptilophorus dufourii* (Dias et al., 2022a).

Sperm features of the ripiphorid *P. fennica* here studied can be summarized as follows: three-layered acrosome, a finding already quoted by Kathirithamby et al. (1993), cylindrical nucleus and a long flagellum with a common 9 + 9+2. The microtubule disorganization occurs only at the tail tip, with only 9 accessory tubules. The diameter of mitochondrial derivatives and accessory bodies is a characteristic that can vary within the group. In *M. tricuspidata* and in *P. dufourii*, mitochondrial derivatives and accessory bodies are thick and similar to those of other Tenebrionidae such as

Tenebrio molitor, *Tribolium castaneum*, *Oedemera nobilis*, *Acanthopus velikensis*, *Mylabris variabilis*, *Mylabris hieracii*, *Hycleus scutellatus* (Nardi et al., 2013; Dias et al., 2015, 2022a, 2022b), while in *Zonitis flava*, they have a quite reduced size (Nardi et al., 2013).

In conclusion, Mordellidae appears to maintain a conserved sperm model, while Ripiphoridae exhibits greater variability. Mordelloidea is morphologically supported at the level of sperm structure by the presence of sperm looping, which is associated with the long sperm predominant in the species. This characteristic is quite distinctive and, together with the fossil record, morphology, and genomic data, supports the position of Mordellidae + Ripiphoridae as a sister lineage to Tenebrionoidea. All tenebrionoid families (sensu Batelka et al., 2025) studied to date exhibit relatively short spermatozoa, organized in bundles within the germinal cysts, with opposite orientation (Dias et al., 2012, 2013a, 2013b, 2015, 2021, 2022a, 2013b, b; Folly et al., 2021, Rezende et al., 2024b).

The limited number of examined species of Mordelloidea, however, suggests to extend the study to other species of this lineage, especially considering that both Mordellidae and Ripiphoridae have differentiated several infra-lineages sometimes with considerable different bionomical traits (Batelka et al., 2025). The same is, however, valid for megadiverse Tenebrionoidea of which only six families and 18 genera were investigated so far.

The cladistic analysis of Mordelloidea and Tenebrionoidea including Mesozoic fossil material (Batelka et al., 2025) revealed that we have to consider in any future evolutionary scenarios also the stem group of Mordelloidea (of which we of course will never have information about soft tissues). More comprehensive information about the sperm arrangement of Lymexyloidea is indeed essential for further discussion. At the moment it seems that looping of the sperm in Mordelloidea is a critical character of high importance in any future evolutionary scenarios of this early split.

CRediT authorship contribution statement

Jan Batelka: Writing – review & editing, Writing – original draft, Resources, Conceptualization. **David Mercati:** Writing – review & editing, Writing – original draft, Visualization, Investigation, Conceptualization. **Mariangela Gentile:** Writing – review & editing, Writing – original draft, Investigation. **Pietro Lupetti:** Writing – review & editing, Writing – original draft, Conceptualization. **Romano Dallai:** Writing – review & editing, Writing – original draft, Methodology, Investigation, Conceptualization.

Declaration of competing interest

The authors declare that they have no known competing financial interests or personal relationships that could have appeared to influence the work reported in this paper.

References

Afzelius, B.A., Dallai, R., 1994. Characteristics of the flagellar axoneme of Neuroptera, Coleoptera, and Strepsiptera. J. Morphol. 219, 15–20. https://doi.org/10.1002/jmor.1052190104.

Almeida, M.C., Cruz-Landim, C., 2000. Spermiogenesis in *Palembus dermestoides* (Coleoptera: Tenebrionidae) with emphasis on the formation of mitochondrial derivatives. Brazilian J. Morphol. Sci. 17, 75–80.

Batelka, J., Kundrata, R., Straka, J., 2025. Phylogenomics and revised classification of Lymexyloidea and Tenebrionoidea (Coleoptera: Polyphaga: Cucujiformia). Syst. Entomol. 1–19. https://doi.org/10.1111/syen.12683.

Beutel, R.G., Friederich, F., 2005. Comparative study of larvae of Tenebrionoidea (Coleoptera: Cucujiformia). Eur. J. Entomol. 102, 241–264. https://doi.org/10.14411/eje.2005.037.

Bocak, L., Barton, C., Crampton-Platt, A., Chesters, D., Ahrens, D., Vogler, A.P., 2014. Building the Coleoptera tree-of-life for >8000 species: composition of public DNA data and fit with Linnaean classification. Syst. Entomol. 39, 97–110. https://doi.org/10.1111/syen.12037.

Bouchard, P., Smith, A.B.T., Douglas, H., Gimmel, M.L., Brunke, A.J., Kanda, K., 2017. Biodiversity of Coleoptera. In: Foottit, R.G., Adler, P.H. (Eds.), Insect Biodiversity: Science and Society, second ed., vol. I. John Wiley & Sons Ltd, Hoboken, NJ, pp. 337–417. https://doi.org/10.1002/9781118945568.ch11.

Cai, C., Tihelka, E., Giacomelli, M., Lawrence, J.F., Ślipiński, A., Kundrata, R., Yamamoto, S., Thayer, M.K., Newton, A.F., Leschen, R.A.B., Gimmel, M.L., Lü, L., Engel, M.S., Bouchard, P., Huang, D., Pisani, D., Donoghue, P.C.J., 2022. Integrated phylogenomics and fossil data illuminate the evolution of beetles. R. Soc. Open Sci. 9, 211771. https://doi.org/10.1098/rsos.211771.

Crowson, R.A., 1955. The Natural Classification of the Families of Coleoptera. Nathaniel Lloyd, London.

Crowson, R.A., 1966. Observations on the constitution and subfamilies of the family Melandryidae (Coleoptera). Eos 41, 507–513.

Dallai, R., 2014. Overview on spermatogenesis and sperm structure of Hexapoda. Arthropod Struct. Dev. 43, 257–290. https://doi.org/10.1016/j.asd.2014.04.002.

Dallai, R., Mercati, D., Lupetti, P., 2024. The ultrastructure of the spermatheca of *Mordellistena brevicauda* (Coleoptera, Tenebrionoidea) and the associated bacterial cells. Arthropod Struct. Dev. 80, 101357. https://doi.org/10.1016/j.asd.2024.101357.

Dias, G., Yotoko, K.S.C., Gomes, L.F., Lino-Neto, J., 2012. Uncommon formation of two antiparallel sperm bundles per cyst in tenebrionid beetles (Coleoptera). Naturwissenschaften 99, 773–777. https://doi.org/10.1007/s00114-012-0949-6.

Dias, G., Oliveira, C.M., Lino-Neto, J., 2013a. Testicular and spermatogenic characteristics of *Lagria villosa* (Tenebrionidae: Lagriinae) with taxonomic inferences. Tissue Cell 45, 227–230. https://doi.org/10.1016/j.tice.2013.03.006.

Dias, G., Oliveira, C.M., Lino-Neto, J., 2013b. Sperm morphology and phylogeny of Lagriids (Coleoptera, Tenebrionidae). Arthropod Struct. Dev. 42, 379–384. https://doi.org/10.1016/j.asd.2013.04.002.

Dias, G., Lino-Neto, J., Mercati, D., Dallai, R., 2015. The sperm ultrastructure and spermiogenesis of *Tribolium castaneum* (Coleoptera: Tenebrionidae) with evidence of cyst degeneration. Micron 73, 21–27. https://doi.org/10.1016/j.micron.2015.03.003.

Dias, G., Lino-Neto, J., Mercati, D., Fanciulli, P.P., Lupetti, P., Dallai, R., 2021. The sperm ultrastructure of *Pytho depressus* (Linnaeus, 1767) (Coleoptera, Pythidae). Micron 148, 103111. https://doi.org/10.1016/j.micron.2021.103111.

Dias, G., Lino-Neto, J., Mercati, D., Fanciulli, P.P., Lupetti, P., Dallai, R., 2022a. The sperm ultrastructure of members of basal Tenebrionoidea(Coleoptera). Arthropod Struct. Dev. 66, 101129. https://doi.org/10.1016/j.asd.2021.101129.

Dias, G., Mercati, D., Rezende, P.H., Lino-Neto, J., Fanciulli, P.P., Lupetti, P., Dallai, R., 2022b. New findings on the sperm structure of Tenebrionoidea (Insecta, Coleoptera). Insects 13, 485. https://doi.org/10.3390/insects13050485.

Folly, C., Pecci-Maddalena, I.S.C., Lopes-Andrade, C., Lino-Neto, J., 2021. The reproductive system of *Ceracis cornifer* (Mellié) and first description of sperm structure in a minute tree-fungus beetle (Tenebrionoidea: Ciidae). Arthropod Struct. Dev. 64, 101088. https://doi.org/10.1016/j.asd.2021.101088.

Forbes, W.T.M., 1926. The wing folding patterns of the Coleoptera. J. N. Y. Entomol. Soc. 34, 42–68. http://www.jstor.org/stable/25004114.

Goczał, J., Beutel, R.G., Gimmel, M.L., Kundrata, R., 2024. When a key innovation becomes redundant: Patterns, drivers and consequences of elytral reduction in Coleoptera. Syst. Entomol. 49, 193–220. https://doi.org/10.1111/syen.12617.

Gunter, N.L., Levkaničová, Z., Weir, T.H., Ślipiński, A., Cameron, S.L., Bocak, L., 2014. Towards a phylogeny of the Tenebrionoidea (Coleoptera). Mol. Phylogenet. Evol. 79, 305–312. https://doi.org/10.1016/j.ympev.2014.05.028.

Hunt, T., Bergsten, J., Levkaničová, Z., Papadopoulou, A., St John, O., Wild, R., Hammond, P.M., Ahrens, D., Balke, M., Caterino, M.S., Gómez-Zurita, J., Ribera, I., Barraclough, T.G., Bocakova, M., Bocak, L., Vogler, A.P., 2007. A Comprehensive Phylogeny of Beetles Reveals the Evolutionary Origins of a Superradiation. Science 318, 1913–1916. https://doi.org/10.1126/science.1146954.

Kathirithamby, J., Carcupino, M., Mazzini, M., 1993. Comparative spermatology of four species of Strepsiptera and comparison with a species of primitive Coleoptera (Rhipiphoridae). Int. J. Insect Morphol. Embryol. 22, 459–470. https://doi.org/10.1016/0020-7322(93)90024-U.

Kheirallah, D.A.M., El-Moaty, Z.A., El-Gendy, D.A., 2016. Impact of cement dust on the testis of *Tachyderma hispida* (Forskal, 1775) (Coleoptra: Tenebrionidae), inhabiting Mariout region (Alexandria, Egypt). J. Entomol. 13, 55–71. https://doi.org/10.3923/je.2016.55.71.

Kheirallah, D.A.M., El-Samad, L., Fahmi, N., Osman, W., 2017. Ultrastructure alterations induced by gamma irradiation in spermiogenesis of the ground beetle, *Blaps sulcata*: reference to environmental radiation protection. Environ. Sci. Pollut. Res. Int. 24, 22102–22110. https://doi.org/10.1007/s11356-017-9869-5.

Lacordaire, T., 1859. Histoire Naturelle des Insectes. Genera des Coléoptéres. Tome 5. Libraire Encyclopédique de Roret, Paris, p. 750.

Lawrence, J.F., Newton, A.F., 1995. Families and subfamilies of Coleoptera with selected genera, notes, references, and data on family names. In: Crowson, A., Pakaluk, J., Ślipiński, S.A. (Eds.), Biology, Phylogeny, and Classification of Coleoptera: Papers Celebrating the 80th Birthday of R. Museum i Instytut Zoologii PAN, Warszawa, pp. 779–1006.

Li, X.-H., Li, R.-F., Hu, F.-J., Zheng, S., Rao, F.-Q., An, R., Li, Y.-H., Liu, D.-G., 2024. Comprehensive phylogenomic analyses revealed higher-level phylogenetic relationships within the Cucujiformia. J. Systemat. Evol. 62, 1–13. https://doi.org/10.1111/jse.13079.

Liu, Y.-Y., Zhou, Z.-C., Chen, X.-S., 2020. Characterization of the complete mitochondrial genome of *Epicauta impressicornis* (Coleoptera: Meloidae) and its phylogenetic implications for the infraorder Cucujiformia. J. Insect Sci. 20, 16.

McKenna, D.D., Wild, A.L., Kanda, K., Bellamy, C.L., Beutel, R.G., Caterino, M.S., Farnum, C.W., Hawks, D.C., Ivie, M.A., Jameson, M.L., Leschen, R.A.B., Marvaldi, A.E., McHugh, J.V., Newton, A.F., Robertson, J.A., Thayer, M.K., Whiting, M.F., Lawrence, J.F., Ślipiński, A., Maddison, D.R., Farrell, B.D., 2015. The beetle tree of life reveals that Coleoptera survived End-Permian mass extinction to diversify during the cretaceous terrestrial revolution. Syst. Entomol. 40, 835–880. https://doi.org/10.1111/syen.12132.

McKenna, D.D., Shin, S., Ahrens, D., Balke, M., Beza-Beza, C., Clarke, D.J., Donath, A., Escalona, H.E., Friedrich, F., Letsch, H., Liu, S., Maddison, D., Mayer, C., Misof, B., Murin, P.J., Niehuis, O., Peters, R.S., Podsiadlowski, L., Pohl, H., Scully, E.D., Yan, E.V., Zhou, X., Ślipiński, A., Beutel, R.G., 2019. The evolution and genomic basis of beetle diversity. Proc Natl Acad Sci USA 116, 24729–24737. https://doi.org/10.1073/pnas.1909655116.

Nardi, J.B., Delgado, J.A., Collantes, F., Miller, L.A., Bee, C.M., Kathirithamby, J., 2013. Sperm cells of a primitive Strepsipteran. Insects 4, 463–475. https://doi.org/10.3390/insects4030463.

Rezende, P.H., Mercati, D., Lupetti, P., Dallai, R., 2024a. The sperm structure of the Scraptiidae (Coleoptera; Tenebrionoidea). Micron 176, 103546. https://doi.org/10.1016/j.micron.2023.103546.

Rezende, P.H., da, S., Paulo, M., Ayala-Costa, D., Texeira, A.G.P., Nascimento, F.W., Alves, M.P., Folly, C., Lino-Neto, J., Dias, G., 2024b. Evidence of antiparallel sperm bundles and limited sperm production in adult males of *Phaleria testacea* Say, 1824 (Tenebrionidae, Diaperinae). Tissue Cell 91, 102621. https://doi.org/10.1016/j.tice.2024.102621.

Robertson, J.A., Ślipiński, A., Moulton, M., Shockley, F.W., Giorgi, A., Lord, N.P., McKenna, D.D., Tomaszewska, W., Forrester, J., Miller, K.B., Whiting, M.F., McHugh, J.V., 2015. Phylogeny and classification of Cucujoidea and the recognition of a new superfamily Coccinelloidea (Coleoptera: Cucujiformia). Syst. Entomol. 40, 745–778. https://doi.org/10.1111/syen.12138.

Shonouda, M., Osman, W., 2018. Ultrastructural alterations in sperm formation of the beetle, *Blaps polycresta* (Coleoptera: Tenebrionidae) as a biomonitor of heavy metal soil pollution. Environ. Sci. Pollut. Res. Int. 25, 7896–7906. https://doi.org/10.1007/s11356-017-1172-y.

Stork, N.E., McBroom, J., Gely, C., Hamilton, A.J., 2015. New approaches narrow global species estimates for beetles, insects, and terrestrial arthropods. Proc Natl Acad Sci USA 112, 7519–7523. https://doi.org/10.1073/pnas.1502408112.

Timmermans, M.J.T.N., Barton, C., Haran, J., Ahrens, D., Culverwell, C.L., Ollikainen, A., Dodsworth, S., Foster, P.G., Bocak, L., Vogler, A.P., 2016. Family-level sampling of mitochondrial genomes in Coleoptera: compositional heterogeneity and phylogenetics. Genome Biol. Evol. 8, 161–175. https://doi.org/10.1093/gbe/evv241.

Virkki, N., 1973. Evolution of sperm cell number per bundle in insects. An. Esc. Nac. Cienc. Biol. México 20, 23–34.

Zhang, S.Q., Che, L.-H., Li, Y., Liang, Dan, Pang, H., Ślipiński, A., Zhang, P., 2018. Evolutionary history of Coleoptera revealed by extensive sampling of genes and species. Nat. Commun. 9, 205. https://doi.org/10.1038/s41467-017-02644-4.